EPJ Web of Conferences **339**, 05007 (2025) https://doi.org/10.1051/epjconf/202533905007
Hard Probes 2024

Electroweak vector-boson production in hadronic collisions with ALICE at the LHC

Shingo Sakai for the ALICE collaboration[1,*]

[1]Tsukuba University of Technology, Faculty of Industrial Technology Amakubo 4-3-15, Tsukuba City, Ibaraki, JPN Zip code:305-8520

Abstract. In the ALICE experiment, the productions of $W^{\pm}$ and Z^0 are studied by exploiting their leptonic decay channels in a wide rapidity region. In this contribution, the differential cross sections for $W^{\pm}$ and Z^0 in proton–proton (pp) collisions at $\sqrt{s}$ = 13 TeV, proton–Pb (p–Pb) collisions at $\sqrt{s_{\mathrm{NN}}}$ = 8.16 TeV and Pb–Pb collisions at centre-of-mass energy of $\sqrt{s_{\mathrm{NN}}}$ = 5.02 TeV are presented. The charged-particle multiplicity dependence of electrons from $W^{\pm}$ bosons and the associated hadrons production in pp collisions at $\sqrt{s}$ = 13 TeV is also shown.

1 Introduction

The $W^{\pm}$ and Z^0 bosons are massive gauge bosons that mediate the weak interaction. In hadronic collisions, $W^{\pm}$ and Z^0 bosons are predominantly produced through quark–antiquark annihilation [1]. As a result, their production cross sections are highly sensitive to the parton distribution functions (PDFs) of up and down quarks in nucleons and nuclei. In proton–proton (pp) collisions, the measurement of $W^{\pm}$ and Z^0 bosons serves as a crucial test of perturbative quantum chromodynamics (pQCD) and electroweak theory. Recent observations in high-multiplicity pp collisions have revealed a faster-than-linear increase as a function of multiplicity increase in charged-hadron production [2], though the underlying mechanism remains an open question. Since $W^{\pm}$ and Z^0 bosons interact only via the weak interaction, their production and behaviour may differ from those of strongly interacting particles, providing complementary insights into the dynamics of these collisions.

In proton–lead (p–Pb) and lead–lead (Pb–Pb) collisions, $W^{\pm}$ and Z^0 bosons offer a means to investigate the nuclear modification of parton distribution functions (nPDFs). Understanding these modifications is essential for characterising initial-state nuclear effects in heavy-ion collisions, which play a key role in the interpretation of quark–gluon plasma signatures.

2 ALICE apparatus and $W^{\pm}$ and Z^0 boson reconstruction

In the ALICE experiment, $W^{\pm}$ and Z^0 boson production is studied by exploiting their decay into electrons at midrapidity and into muons at forward rapidity. The details of the detector and its performance are described in Ref. [3].

*e-mail: sakai.shingo.gw@alumni.tsukuba.ac.jp

At midrapidity, the $W^{\pm}$ and Z^0 boson candidates are reconstructed by measuring the electrons from their leptonic decays with the Time Projection Chamber (TPC) and the Electromagnetic Calorimeter (EMCal). The electrons are identified based on their energy loss ($\mathrm{d}E/\mathrm{d}x$) in the TPC, and on the energy-to-momentum ratio ($E/p \sim 1$), where the energy is measured in the EMCal and the momentum is measured in the TPC. An isolation criterion is applied on the energy information around the electron candidates to separate $W^{\pm}$ and Z^0 bosons from hadron decays. Z^0 bosons are reconstructed computing the invariant mass of the two identified electrons of opposite sign.

At forward rapidity, the $W^{\pm}$ boson candidates are reconstructed in the single-muon channel with the muon spectrometer. The yield of muons from $W^{\pm}$ boson decay is extracted by fitting the measured single-muon transverse momentum spectrum ($p_{\mathrm{T}}^{\mu} > 10$ GeV/c) with the templates obtained with Monte Carlo simulations including background from Z^0 boson and heavy-flavour hadron decays. The templates were computed by the POWHEG event generator [4] for muons from $W^{\pm}$ and Z^0 boson decays and fixed-order plus next-to-leading log (FONLL) perturbative QCD calculations [5, 6] for heavy-flavour hadrons. In the POWHEG simulations for p–Pb and Pb–Pb collisions, the lead nucleus isospin is taken into account by weighting the proton and neutron contributions. The Z^0 bosons are reconstructed with an invariant mass analysis in the dimuon decay channel $Z^0 \rightarrow \mu^+\mu^-$ with $p_{\mathrm{T}}^{\mu} > 20$ GeV/c in the rapidity range $2.5 < y < 4$.

3 Results

3.1 $W^{\pm}$ and Z^0 production in pp collisions at $\sqrt{s}$ = 13 TeV

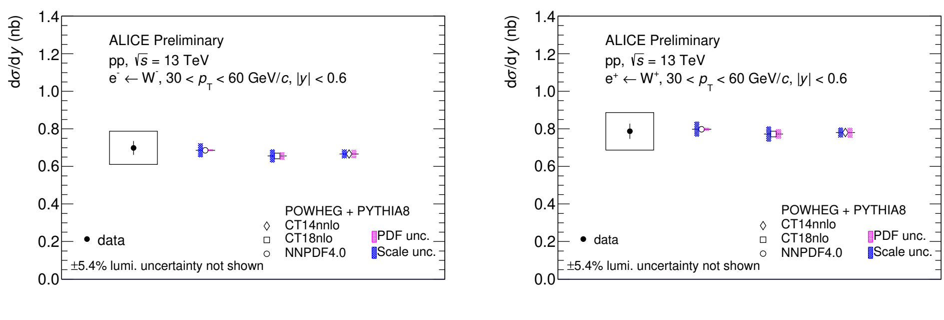

Figure 1. Production cross section of electrons from W^- (left) and positrons from W^+ (right) decays at midrapidity in pp collisions at $\sqrt{s}$ =13 TeV, compared with POWHEG calculations with the CT14nnlo [7], CT18nlo [8], and NNPDF4.0 [9] PDF sets. The production cross sections are obtained by integrating $e^{\pm} \leftarrow W^{\pm}$ in the interval $30 < p_{\mathrm{T}} < 60$ GeV/c.

The transverse momentum integrated cross sections for electrons originating from $W^{\pm}$ boson decays ($30 < p_{\mathrm{T}} < 60$ GeV/c) are shown in Fig. 1. The results for electrons from W^- decays are presented on the left, while those for positrons from W^+ decays are shown on the right. The measured cross sections are compared with theoretical predictions based on pQCD calculations at next-to-leading order (NLO), obtained using the POWHEG framework [4]. The comparisons include predictions employing different PDFs, specifically CT14nnlo [7], CT18nlo [8], and NNPDF4.0 [9]. The experimental results are consistent with the theoretical calculations within uncertainties.

Figure 2 shows the self-normalised yields of electrons from $W^{\pm}$ bosons and charged hadrons in association with $W^{\pm}$ bosons as a function of normalised charged-particle multiplicity at midrapidity in pp collisions at $\sqrt{s} = 13$ TeV. The production of electrons from $W^{\pm}$ bosons is linear with respect to the multiplicity. On the other hand, this trend of the associated hadron production is faster than linear. The trend has several interpretations, and one possible explanation is the auto-correlation between the measured hadrons and the charged multiplicity [11]. In contrast, $W^{\pm}$ bosons show a linear trend as they are less correlated with multiplicity. The result is compared with PYTHIA8 predictions [10] including multiparton interactions (MPI) and colour reconnection (CR), which describe the measurements within uncertainties.

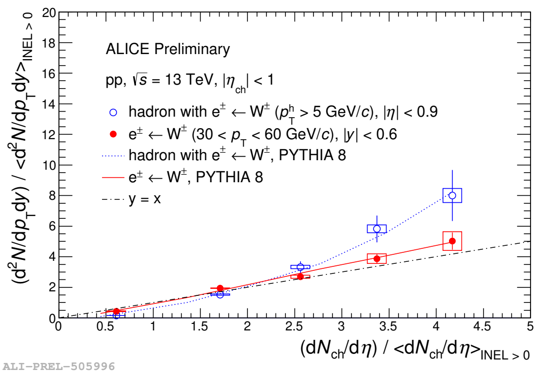

Figure 2. Self-normalised yields of $e^{\pm} \leftarrow W^{\pm}$ and associated hadrons vs. normalised charged-particle pseudorapidity density compared with expectations from PYTHIA8 [10] simulation including CR effects.

The fiducial cross section of Z^0 bosons is measured under specific kinematic conditions. One of the decay electrons or positrons is required to have a transverse momentum greater than 30 GeV/c and a rapidity of less than 0.6. Z^0 bosons are reconstructed using their invariant mass. The invariant mass distribution of e^+e^- pairs is shown in Fig. 3 (left). The invariant mass of the dilepton system is selected within the range of 60–108 GeV/c^2. The fiducial cross section of Z^0 bosons is shown in Fig. 3 (right) and compared with POWHEG calculations incorporating CT14nnlo [7], CT18nlo [8], and NNPDF4.0 [9] PDFs. The comparison demonstrates that these theoretical models, which have shown good agreement with W boson production data at midrapidity, also describe the measured Z^0 boson fiducial cross sections well within the experimental uncertainties.

3.2 $W^{\pm}$ production in p–Pb and Pb–Pb collisions

Figure 4 presents the ratio between the production cross section of $W^{\pm}$ bosons measured by the ALICE [12] and CMS [13] collaborations in p–Pb collisions at $\sqrt{s_{NN}} = 8.16$ TeV and the predictions from NLO pQCD calculations using the CT14 PDFs [7] as a function of rapidity. The CMS experiment measured W boson production via the muonic decay channel, covering rapidities up to approximately $|y| < 2.0$. ALICE extends the rapidity coverage beyond that of CMS, reaching larger rapidities. The ALICE measurements are consistent with the trend observed at the edges of the CMS acceptance and provide further evidence for the suppression

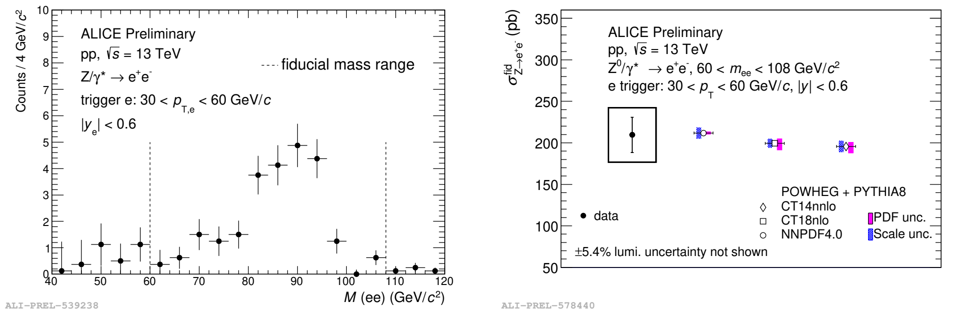

Figure 3. Invariant mass distribution of dielectrons from Z^0 decay (left) and fiducial cross section of the reconstructed Z^0 bosons (right) in pp collisions at $\sqrt{s} = 13$ TeV.

of $W^{\pm}$ boson production at large rapidity. These results support the presence of significant nuclear modifications to the parton distribution functions in heavy-ion collisions.

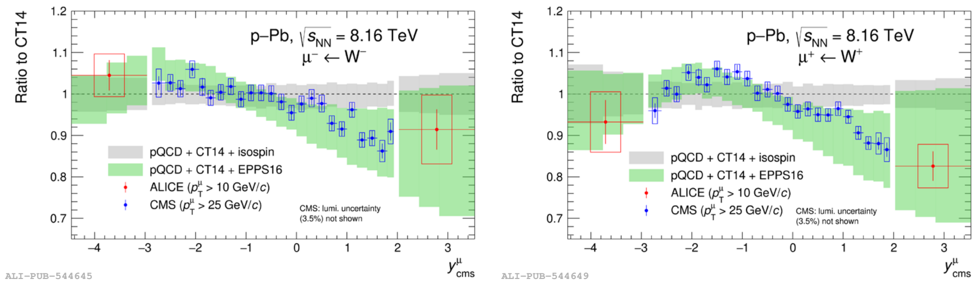

Figure 4. Ratio between the production cross section of $W^{\pm}$ boson measured in ALICE [12] and CMS [13] collaboration in p–Pb collisions at $\sqrt{s_{\mathrm{NN}}} = 8.16$ TeV and predictions from NLO pQCD calculations using the CT14 PDFs [7] as a function of rapidity.

Figure 5 shows the rapidity dependence of $W^{\pm}$ boson production in Pb–Pb collisions at $\sqrt{s_{\mathrm{NN}}} = 5.02$ TeV, as measured by the ALICE [12] and ATLAS [14] experiments. ATLAS has performed measurements in both the electronic and muonic decay channels, covering rapidities up to $|y| < 2.4$. In this analysis, the ratio of the experimental results from ALICE and ATLAS to NLO pQCD calculations is shown as a function of rapidity. The ALICE measurements extend the rapidity coverage beyond that of ATLAS. The results obtained by ALICE are well described by calculations incorporating EPPS16 nuclear parton distribution functions (nPDFs) [15], while predictions based on the CT14 free-proton PDFs (without EPPS16) overestimate the data by approximately 2σ. However, the EPPS16-based calculations underestimate the ATLAS measurements. At large rapidities, the ratio of experimental results to CT14 predictions falls below unity, indicating a significant modification of the parton distribution functions in the nuclear environment. These observations highlight the importance of precise nPDF constraints in the forward rapidity region.

3.3 Z^0 production in p–Pb and Pb–Pb collisions

The production cross section of Z^0 bosons decaying into $\mu^+\mu^-$ in p–Pb collisions at $\sqrt{s_{\mathrm{NN}}} = 8.16$ TeV [16] is shown in Fig. 6 (left). The production was measured in two rapidity ranges

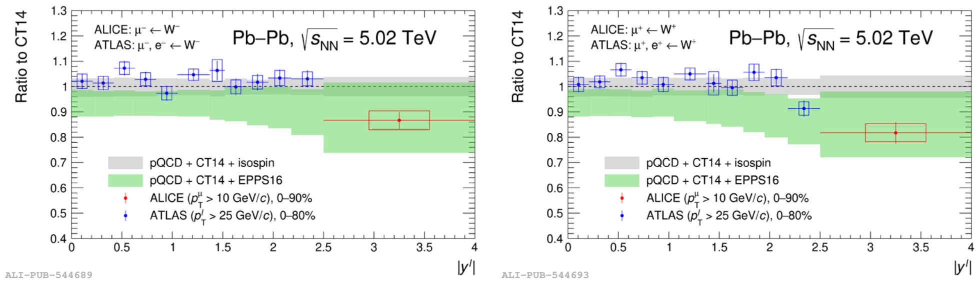

Figure 5. Ratio to CT14 predictions [7] of the production of muons from W^- (left) and W^+ (right) decays measured in Pb–Pb collisions at $\sqrt{s_{NN}}$ = 5.02 TeV by the ALICE [12] and ATLAS [14] Collaborations.

$2.03 < y < 3.35$ and $-4.46 < y < -2.96$. The results are compared with pQCD-based models, MCFM [17] and FEWZ [18], that account for isospin effects, both with and without EPPS16 nPDFs. Within the experimental and theoretical uncertainties, the models show good agreement with the measured cross sections with and without the nPDFs. The production cross section of Z^0 bosons decaying into $\mu^+\mu^-$ in Pb–Pb collisions at $\sqrt{s_{NN}}$ = 5.02 TeV [16] is shown in Fig. 6 (right). The result is normalised by the nuclear overlap function. The result is also compared with the theoretical calculations based on MCFM and FEWZ with and without nuclear PDFs (EPPS16, nCTEQ15 [19] and EPS09s [20]). The calculations with nuclear PDFs are in good agreement with the data. On the other hand, the calculation without the nuclear modification (MCFM + CT14) is 3.4σ higher than the data.

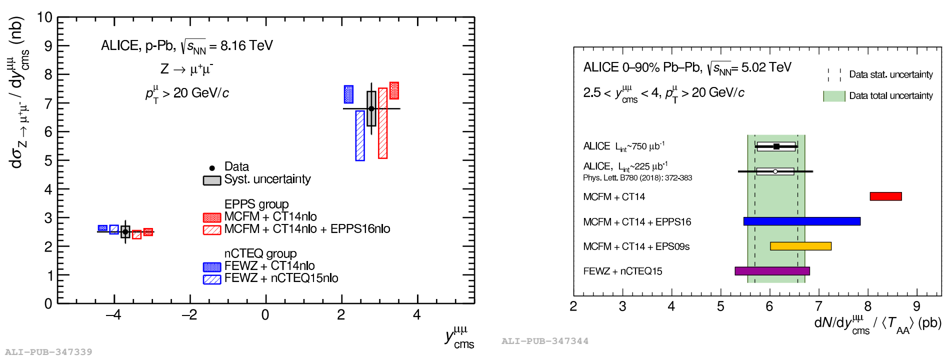

Figure 6. (Left) Production cross section of $Z^0 \rightarrow \mu^+\mu^-$ in p–Pb collisions at $\sqrt{s_{NN}}$ = 8.16 TeV [16]. (Right) Invariant yield of $Z^0 \rightarrow \mu^+\mu^-$ divided by the nuclear overlap function in Pb–Pb collisions at $\sqrt{s_{NN}}$ = 5.02 TeV [16].

4 Summary

The production of $W^\pm$ and Z^0 bosons was measured with the ALICE experiment in pp collisions at $\sqrt{s}$ = 13 TeV, p–Pb collisions at $\sqrt{s_{NN}}$ = 8.16 TeV, and Pb–Pb collisions at $\sqrt{s_{NN}}$ = 5.02 TeV using datasets collected during the LHC Run 2 data-taking period. In pp collisions, the measured cross sections for $e^\pm \leftarrow W^\pm$ and $Z^0 \rightarrow e^+e^-$ are in good agreement with theoretical predictions based on pQCD including PDFs. The production of $W^\pm$ bosons at midrapidity shows an increasing linear trend as a function of charged-particle multiplicity. In p–Pb collisions, the rapidity dependence of $\mu^{\pm} \leftarrow \mathrm{W}^{\pm}$ was measured. The measurements were compared with models with and without nuclear modification of the PDFs, and significant deviation between data and models were found at large rapidity in the forward region. In Pb–Pb collisions, $\mu^{\pm} \leftarrow \mathrm{W}^{\pm}$ and $\mathrm{Z}^{0} \rightarrow \mu^{+}\mu^{-}$ were measured at forward rapidity. The $\mathrm{W}^{\pm}$ and Z^{0} boson production cross sections measured in forward rapidity are in good agreement with models that include nuclear effects, which suggests a significant modification of the nuclear PDFs.

References

[1] M. Schott and M. Dunford, EPJ. C **74** (2014), 2916.
[2] S. Acharya *et al.* [ALICE], PLB **810** (2020), 135758.
[3] K. Aamodt *et al.* [ALICE], JINST **3** (2008), S08002.
[4] S. Alioli, P. Nason, C. Oleari and E. Re, JHEP **07** (2008), 060.
[5] M. Cacciari, M. Greco and P. Nason, JHEP **9805** (1998) 007.
[6] M. Cacciari, S. Frixione and P. Nason, JHEP **0103** (2001) 006.
[7] S. Dulat *et al.*, PRD **93**, no.3, 033006 (2016)
[8] M. Yan, T. J. Hou, P. Nadolsky and C. P. Yuan, PRD **107**, no.11, 116001 (2023)
[9] R. D. Ball *et al.* [NNPDF], EPJ. C **82**, no.5, 428 (2022)
[10] T. Sjöstrand *et al.*, Comput. Phys. Commun. **191**, 159-177 (2015)
[11] S. G. Weber, A. Dubla, A. Andronic and A. Morsch, EPJ. C **79**, no.1, 36 (2019)
[12] S. Acharya *et al.* [ALICE], JHEP **05**, 036 (2023)
[13] A. M. Sirunyan *et al.* [CMS], PLB **800**, 135048 (2020)
[14] G. Aad *et al.* [ATLAS], EPJ. C **79**, no.11, 935 (2019)
[15] K. J. Eskola, P. Paakkinen, H. Paukkunen and C. A. Salgado, EPJ. C **77**, no.3, 163 (2017)
[16] S. Acharya *et al.* [ALICE], JHEP **09**, 076 (2020)
[17] J. Campbell and T. Neumann, JHEP **12**, 034 (2019)
[18] R. Gavin, Y. Li, F. Petriello and S. Quackenbush, Comput. Phys. Commun. **182**, 2388-2403 (2011)
[19] A. Kusina *et al.*, EPJ. C **77**, no.7, 488 (2017)
[20] I. Helenius, K. J. Eskola, H. Honkanen and C. A. Salgado, JHEP **07**, 073 (2012)